Research Journal of Environmental Sciences 5 (4): 329-341, 2011
ISSN 1819-3412 / DOI: 10.3923/rjes.2011.329.341

A Comparative Study of the Preliminary Examining Methods for Liquefaction Potential and Geological Conditions of Coastal Soils in the Southeastern Caspian Sea

[1]H. Rezaiy, [1]G.R. Lashkaripour, [1]M. Ghafouri and [2]N.H. Mogaddas
[1]Department of Engineering Geology, Ferdowsi University of Mashhad, Iran
[2]Department of Engineering Geology, Shahroud University, Iran

Corresponding Author: Hamed Rezaiy, Department of Engineering Geology, Ferdowsi University of Mashhad, Iran

ABSTRACT

Liquefaction is one of the most common damaging phenomena and its importance has motivated research. Various methods have been recommended by investigators to analyze liquefaction potential, each of which may be used depending on the quantifiable data and geological conditions. In this study, the liquefaction potential of a foundation soil in the city of Bandar Torkaman, situated in Southeastern part of the Caspian Sea (Golestan Province, Iran) was studied using multiple methods. The geological conditions and soil deposition state were assessed in this region and the influence of geological conditions on liquefaction potential was investigated as well. The obtained results show a relatively close correlation between the liquefaction potential and standard penetration test results, relative density and Atterberg limits. Furthermore, the Casagrande test, which is used for the determination of fine-grained soil liquid limits, displayed, to some extent, dynamic soil behavior. There is also a very close relationship between a soil's Liquid Limit (LL) and the factor of safety derived from the cyclic stress ratio. Finally, from a theoretical point of view, it is possible that soil may meet criteria for possible liquefaction, but it can be influenced by different interrelated geological factors.

Key words: Liquefaction, engineering geology, geotechnique, earthquake

INTRODUCTION

Liquefaction occurs during heavy shaking by earthquakes, when the pressure exerted by the water in saturated soil causes soil particles to become suspended in the water. A soil deposit that is liquefied behaves like quicksand (Alisha, 2004). In other words, liquefaction results in diminished ground strength due to increased water pressure in saturated soils resulting from cyclic stress. Liquefaction is one of the most prevalent hazardous phenomena in coastal areas and is most likely to occur as a consequence of earthquakes (Idriss and Boulanger, 2003).

Ground motion characteristics, soil type and in situ stress conditions constitute the three primary factors in the development of cyclic mobility or liquefaction (Department of Defense, 1983; Idriss and Boulanger, 2003).

In addition, geological factors simultaneously influence the soil's propensity toward liquefaction. These include soil type, relative density (D_r) (Anderson *et al*., 2005), soil gradation (Al-Karni, 2007), the history and condition of the depositing environment (Mirhosainy and Arefpoor, 2001), the

Fig. 1: Location of the area under study in the Southeastern Caspian Sea (Iran)

shape and cementation of soil grains, stratigraphy and drainage conditions (Idriss and Boulanger, 2004). Microstructure properties may be measured to determine liquefaction potential as well (Mihai *et al.*, 2010).

For this paper, the study area consisted of a soil foundation underlying the residential buildings of the Maskan Mehr Housing Project, located in the city of Torkaman, Golestan province, in the North of Iran. The area is located about 200 m away from the coast of the Gorgan Gulf (in the Southeastern part of the Caspian Sea). The geographical coordinates of the above-mentioned area are 36°, 52', 31" E and 54°, 03', 45" N (Fig. 1).

MATERIALS AND METHODS

The results of the studies conducted by Jouya Pars Shomal Consulting Engineers were examined for this study. The geotechnical explorations of the Maskan Mehr Housing Project in Torkaman city occurred between July 13th, 2009 and Feb 6th, 2010. The results of this company's work were summarized in a 170-page report under the project code 2301. A copy of the presented report was given to the authors to conduct the present research (JPSCO, 2010).

Six 15 m deep boreholes and one 25 m deep borehole were drilled in a 4 ha area using a SKB4 drilling machine. The results of the boreholes labeled BH_1, BH_2, BH_3, BH_6 and BH_7 were used for this research (Table 1). All of the tests were performed according to ASTM standards.

Seismicity potential of area: The seismicity history and specifications of active faults in this area are indicative of high seismicity.

Khazar Fault is the most outstanding tectonic feature in this area and has caused great changes in the morphology of the region. The surface trace of the fault is nearly 454 km in length and serves as a border between the mountain and its adjacent plain. The fault has been given different names at different locations, in accordance with the names of the local areas. The relatively frequent occurrence of intermediate- to large-scale earthquakes is among the seismotectonic features of this region. The epicenters of many historical and mechanism earthquakes correspond to the Khazar fault zone.

Table 1: Descriptive information about the study area and the number of samples selected

Type	SPT (N)	Grain size analysis	Specific gravity (Gs)	Plasticity index (PI)	Liquid limit (LL)	Density (γ)	No. of Borehole	Drilling depth (m)
Tested	49	23	41	37	37	40	7	115
Selected	28	14	28	28	28	28	5	84

Table 2: Results of calculations relating to liquefaction potential in different depths of selected boreholes

Borehole No.	Depth (m)	N (SPT)	γ_d -----(g cm^{-3})------	γ_{sat}	G_s	r_d	t_{cyc} (kg cm^{-2})	CSR	PI (%)	σ_{v0} ------(kg cm^{-2})------	σ'_{v0}	CRR	FS	Liquefiable liquefiable
BH_1	3	9	1.53	1.96	2.7	0.977	0.087	0.303	4	0.459	0.289	0.189	0.63	Possible
	6	4	1.31	1.82	2.69	0.954	0.146	0.296	9.6	0.786	0.494	0.240	0.81	Possible
	9	67	1.52	1.95	2.69	0.931	0.248	0.289	21.4	1.368	0.859	0.588	2.03	Impossible
	12	53	1.48	1.93	2.67	0.908	0.315	0.283	4	1.776	1.111	0.207	0.73	Possible
	15	6	1.37	1.87	2.74	0.774	0.310	0.238	4	2.055	1.305	0.182	0.77	Possible
BH_2	3	10	1.36	1.85	2.67	0.977	0.078	0.305	4	0.408	0.255	0.188	0.62	Possible
	6	23	1.37	1.88	2.79	0.954	0.153	0.290	7.7	0.822	0.527	0.225	0.78	Possible
	9	37	1.48	1.94	2.74	0.931	0.242	0.286	8.8	1.332	0.846	0.250	0.88	Possible
	12	12	1.43	1.90	2.7	0.908	0.304	0.281	4	1.716	1.080	0.191	0.68	Possible
	15	8	1.38	1.87	2.69	0.774	0.312	0.240	14.2	2.070	1.300	0.354	1.47	Impossible
BH_3	3	24	1.36	1.86	2.71	0.977	0.078	0.302	4	0.408	0.257	0.197	0.65	Possible
	6	20	1.39	1.89	2.76	0.954	0.155	0.292	4	0.834	0.532	0.195	0.67	Possible
	9	62	1.45	1.92	2.73	0.931	0.237	0.287	4	1.305	0.827	0.208	0.73	Possible
	12	12	1.38	1.87	2.68	0.908	0.293	0.283	4	1.656	1.038	0.190	0.67	Possible
	15	9	1.38	1.86	2.65	0.774	0.312	0.242	4	2.070	1.289	0.187	0.77	Possible
BH_6	3	29	1.43	1.89	2.63	0.977	0.082	0.307	4	0.429	0.266	0.200	0.65	Possible
	6	46	1.53	1.95	2.64	0.954	0.171	0.299	16.1	0.918	0.570	0.426	1.42	Impossible
	9	35	1.57	1.98	2.67	0.931	0.257	0.290	24.1	1.413	0.884	0.669	2.31	Impossible
	12	20	1.44	1.88	2.56	0.908	0.306	0.291	4	1.728	1.053	0.197	0.68	Possible
	15	28	1.59	1.99	2.64	0.774	0.360	0.243	8.4	2.385	1.482	0.243	1.002	Impossible
BH_7	3	51	1.4	1.88	2.71	0.977	0.080	0.302	4	0.420	0.265	0.205	0.68	Possible
	6	7	1.4	1.88	2.68	0.954	0.156	0.297	6.1	0.840	0.527	0.195	0.66	Possible
	9	35	1.49	1.93	2.65	0.931	0.243	0.292	18	1.341	0.835	0.476	1.63	Impossible
	12	11	1.47	1.91	2.62	0.908	0.312	0.286	4	1.764	1.091	0.191	0.67	Possible
	15	8	1.47	1.91	2.64	0.774	0.333	0.243	11.7	2.205	1.370	0.294	1.21	Impossible
	18	8	1.4	1.87	2.63	0.693	0.341	0.218	16.2	2.52	1.562	0.408	1.87	Impossible
	21	10	1.47	1.90	2.6	0.613	0.369	0.194	14.1	3.087	1.900	0.355	1.83	Impossible
	24	12	1.5	1.93	2.63	0.533	0.374	0.168	24.6	3.6	2.231	0.674	4.02	Impossible

According to past seismic activities in the region, the maximum horizontal acceleration of the project (located in Torkaman city) is equal to 0.3 g with a moment magnitude of 7.5. The rupture zone that is closest to the site is at an estimated surface distance of 5 to 10 km.

Methods of liquefaction potential assessment: Comparing the Cyclic Stress Ratio (CSR) with the cyclic resistance ratio (CRR).

Using the following equation, Eq. 1, the cyclic stress ratio resulting from an earthquake, known as the seismic stress ratio (Maugeri and Mouaco, 2006) is obtained at different depths in the drilled boreholes; the calculated results are shown in Table 2.

$$CSR = \frac{\tau_{cyc}}{\sigma_{v0}} = 0.65 r_d \left(\frac{\sigma_{v0}}{\sigma'_{v0}}\right)\left(\frac{\alpha_{max}}{g}\right) \quad (1)$$

There are different methods of calculating the CRR to analyze the results of field experiments (Idriss and Boulanger, 2004). The CRR is a function of the scale factors for earthquake magnitude, effective overburden stresses and ground slope (Anderson *et al.*, 2005).

The results of Standard Penetration Tests (SPT) were also used for the study area. According to Al-Karni (2007), whenever the percent of fine grains of the soil exceeds 35%, the CRR can be calculated from Eq. 2:

$$CRR = 0.065 - 0.234\,PI^{0.5} + 0.057\,PI + 0.34\,[e0/N]^{-0.028} \quad (2)$$

The factor of safety can be obtained from examining the ratio of CRR to CSR. In critical conditions, liquefaction has a quantity equal to one and in depths where the quantity of the safety factor is less than one, there is the potential for liquefaction (Table 2).

Critical void ratio (e_c): Casagrande (1963) demonstrated that all specimens tested at a similar confining pressure, reach to an identical density while failing as a result of large strains and their shear failure continues with the same shear stress. The void ratio corresponding to this constant density is called critical void ratio (e_c), the value of which is dependent on the effective lateral pressure (Mirhosainy and Arefpoor, 2001).

In order to investigate the liquefaction potential based on the critical void ratio, triaxial testing is required. Accordingly, one triaxial test has been done on a specimen gained from BH2 (depth: 6 m). The applied confining pressures were as 0.5, 1.0 and 1.5 kg cm^{-2}. Based on the effective stress in the depth of 6 m, soil void ratio has been calculated and has been put above the critical void ratio curve showing the liquefaction potential of the soil (Fig. 2).

As per Fig. 3, when shear stress is equal to zero during an earthquake, the following relationship is validated, as in Eq. 3.

$$\gamma_{sub.}\, z = \gamma_w h_w \quad (3)$$

where, $\gamma_{sub.}$ and γ_w are the specific weights of suspended soil and water, respectively.

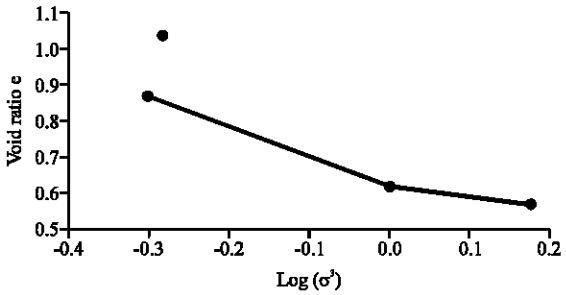

Fig. 2: Assessment of soil liquefaction potential on the basis of critical void ratio in triaxial testing

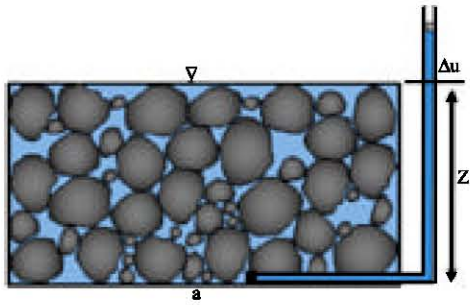

Fig. 3: Liquefaction mechanism

Based on Eq. 4, it can be induced that complete soil failure and liquefaction has occurred as long as the water height is equal to the depth (z) of the submerged soil layer. In such a situation, the following relationship exists:

$$\frac{Gs-1}{1-e}=i_{cr} \tag{4}$$

where, G_s, e and i_{cr} are the soil density, void ratio and critical hydraulic gradient, respectively. Based on the above discussions, $i_{cr}=0$ is the liquefaction threshold and, liquefaction takes place when $i_{cr}>1$.

At the liquefaction threshold state, it can be written that:

$$G_s-1=1+e \rightarrow e_c=G_s-2 \tag{5}$$

The liquefaction potential may be assessed by comparing the initial void ratio (i.e., e_0 obtained from the results of soil mechanic tests (Table 1) and the critical void ratio (i.e., e_c which is calculated by using Eq. 6). Comparing the 27 specimens, it is evident that there is a linear relationship between e_c and e_0, the correlation coefficient of which is r = 0.647 (Fig. 4).

$$e_c=0.3118e_0+0.4056 \tag{6}$$

Boulanger (2002) proposed a relationship between the critical void ratio and the mean effective normal stress.

Comparing the initial and critical void ratios, one can see that the quantity of the initial void ratio was always greater than that of critical void ratio in all of the samples. This indicates that the soil has critical voids at all depths and is consequently susceptible to liquefaction (Fig. 5). On the contrary, the assessments done using other methods did not show liquefaction potential at all depths (Fig. 5). Therefore, it can be induced that high porosity alone cannot determine a soil's liquefaction level.

Grain size distribution: Poorly-graded soils have more porosity compared to well-graded soils. As a result, they are more susceptible to liquefaction.

In order to primarily investigate the liquefaction potential, the size and gradation of soil particles can be used. It is worth indicating that gradation cannot be singly used for liquefaction

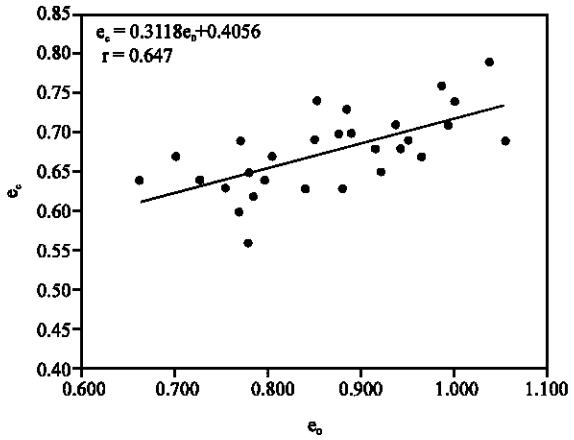

Fig. 4: Relations between the preliminary void ratio (e_0) and the critical void ratio (e_c)

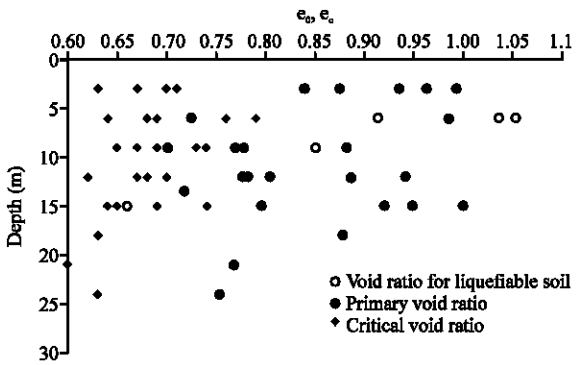

Fig. 5: Comparisons between preliminary and critical void ratios at different depths of selected boreholes

assessment; but other geological parameters such as the form of particle placement next to each other, cementation intensity, surface shape of the particles and connectivity of voids are of great importance as well.

In this research, by placing D50 of the soil in the gradation range, it became evident that some of the specimens had potential for liquefaction (Fig. 6).

Relative density (D_r): Relative density (D_r) is a significant factor in the assessment of liquefaction potential and it has been used by different researchers in various ways (Anderson *et al*., 2005). The relationship between relative density and liquefaction potential is inverse in nature. It is worthwhile to indicate that relative density is calculated in relation to the horizontal stress index (K_D). Comparative studies have indicated that K_D is noticeably reactive to factors such as stress state/history (σ_h, OCR), pure presenting, aging, cementation and structure, all of which increase liquefaction resistance (Maugeri and Monaco, 2006).

The relative soil density is assessed with experimental methods in a laboratory or in field scale. Based on the suggestions of Boulanger and Idriss (2004) the value of relative density was calculated in relation to the standard penetration number (N) and load effective pressure (σ') as follows:

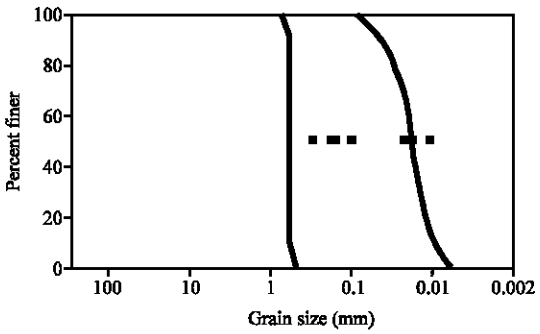

Fig. 6: Location of D50 at different depth samples of boreholes in sheath of liquefaction gradation

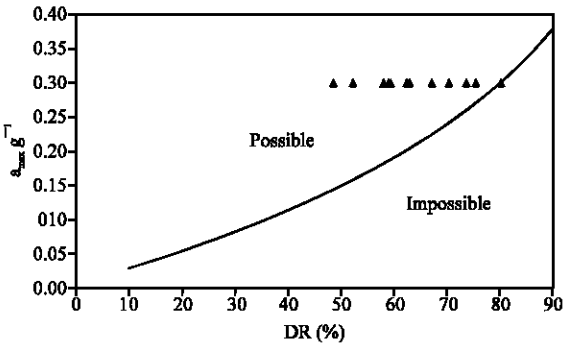

Fig. 7: Assessment of liquefaction potential using maximum acceleration and relative density (Tahooni, 1996)

$$D_r = 25\,\sigma'^{-0.12}N^{0.46} \tag{7}$$

$$\sigma_0' = \Sigma\gamma h \tag{8}$$

The above equation, Eq. 7, shows that the effective stress value is the product of the specific weight of the soil and its height (overburden soil column).

In addition to the calculation in Eq. 9, relative density can be calculated in relation to the mean effective normal stress (Boulanger and Idriss, 2004). Robertson (2007) has also suggested the following relationship for the calculation of D_R (Robertson, 2007).

$$DR = (N/46)^{0.5} \tag{9}$$

After the prediction of D_R from the above equations Eq. 7 and 9, all of the predicted values were put in the diagram in Fig. 7, based on a seismic acceleration of 0.3 g. As is evident, all of the results were located within the limits of possible liquefaction.

Type of deposit: Deposition environment, age of deposit, structure and texture of sediments at the time of deposition and the amount of cementation and interlocking of particles, are all effective factors in the occurrence of liquefaction.

Table 3: Estimated susceptibility of sedimentary deposits to liquefaction during strong seismic shaking based on geologic ages for coastal zones (Mirhosainy and Arefpoor, 2001)

	Likelihood that cohesion less sediments, when saturated, would be susceptible to liquefaction (by age of deposit)			
Type of deposit	<500 years High	Holocene Moderate	Pleistocene Low	Pre-Pleistocene Very low
soils studied	*	*		

According to the fact that the study area is in the Caspian Sea's coastline and based on the geological maps of the area, the sediments are determined as Holocene alluviums with an age less than 500 years. Surface layers with depths up to 3 m are aged less than 500 years and are influenced by tide, while more deep sediments can be categorized as Holocene sediments.

Mirhosainy and Arefpoor (2001) posited that liquefaction potential is dependent on the soils' geological conditions at the time of deposition as well as their ages. In Table 3, the liquefaction potential for the deposits in the study area (related to depositing environments of coastal regions) with ages younger than Holocene were estimated as high to intermediate (Mirhosainy and Arefpoor, 2001).

Results of Standard Penetration Test (SPT): According to the results of a standard penetration test and the effective stress of the granular soil, the boundary between the soil potential to liquefaction and stable soil was determined (Idriss and Boulanger, 2003). By inserting the data gained from the results of the boreholes in Fig. 8, it can be seen that all samples demonstrated potential for liquefaction. In Fig. 9, most of the investigated samples were located in the zone corresponding to liquefaction potential.

The required improvements such as hammer modification coefficients, the length of sampling rod and regulation of the overburden effective pressure on initial values of standard penetration number have been applied and then used in Fig. 8 and 9.

Using plasticity properties and moisture: Liquefaction potential can also be evaluated based on the plasticity diagram derived from the Chinese standard (Al-Karni, 2007).

Sand-like soils are susceptible to cyclic liquefaction when their behavior is characterized by plasticity indices (PI)< 12, Liquid Limits (LL) < 37 and natural water contents (wc)>0.8 (LL) (Robertson, 2007). Polito (1999) has also suggested liquid limits with PI< 10 and LL< 30 as suitable criteria (Polito, 1999).

In Fig. 10, when plotting the samples, it can be observed that the results fall outside of the A and B zones. Moreover, no IP samples were shown with number 4 (Table 2).

Anderson *et al.* (2005) have used the diagram drawn in Fig. 11 for the assessment of liquefaction potentials of the Fraser River Delta silt. In Fig. 11, the y-axis indicates the plasticity index (PI) and the x-axis indicates the relationship between the natural moisture (wc) and liquid limit (LL) values. Twelve specimens from different depths of the were situated in the diagram to visualize liquefaction potential. It was found that three samples were located in the zone susceptible to liquefaction or cyclic mobility, three samples were located in the zone of moderate susceptibility to liquefaction or cyclic mobility and the remaining samples were located in the not susceptible zone. The results of this method correspond to the results of the methods mentioned in Table 2.

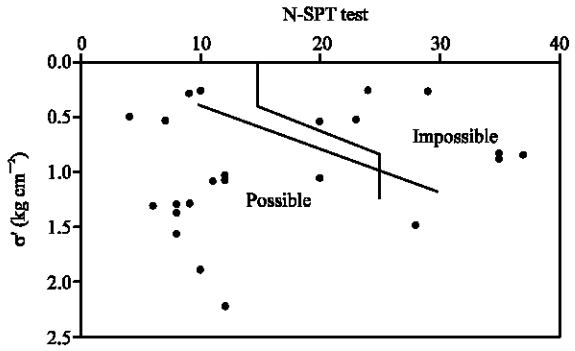

Fig. 8: Assessment of liquefaction potential in relation to effective stress- SPT (Mirhosainy, 1993)

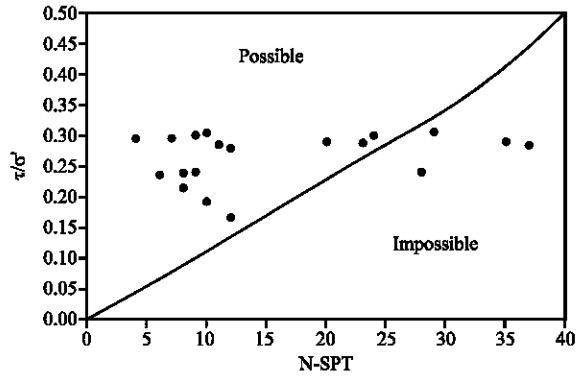

Fig. 9: Limits of soil liquefaction in relation in SPT number with relations of shear stress to effective stress (Mirhosainy, 1993)

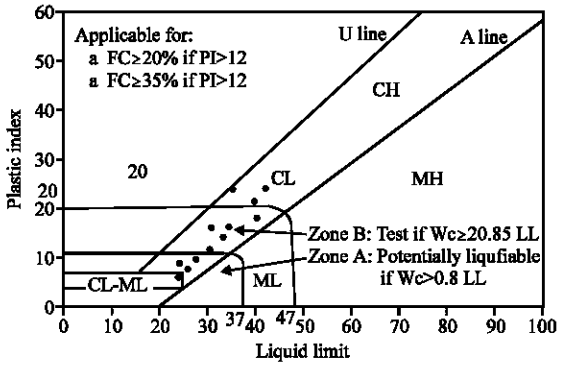

Fig. 10: Assessment of liquefiable soil types (Robertson, 2007), studied region

Application of distance from site to effective epicenter (R): The assessment of an area's liquefaction potential is feasible within a specific distance from the seismic event (Balideh *et al.*, 2009). Using data from low-depth earthquakes that have occurred across the world, Mirhosainy (1993) obtained a critical surface epicenter distance for liquefaction (Fig. 12), beyond which soil is unlikely to liquefy as a consequence of an earthquake (Mirhosainy,1993).

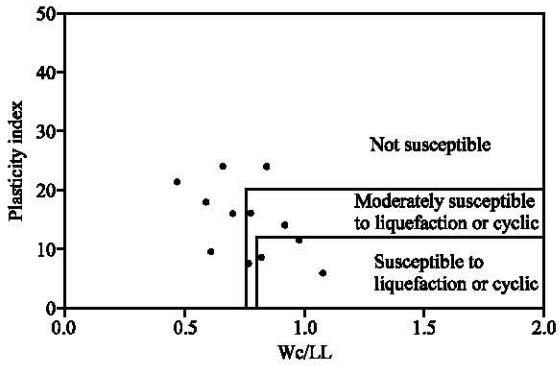

Fig. 11: Liquefaction susceptibility of studied soils based on specific criteria (Anderson *et al*., 2005)

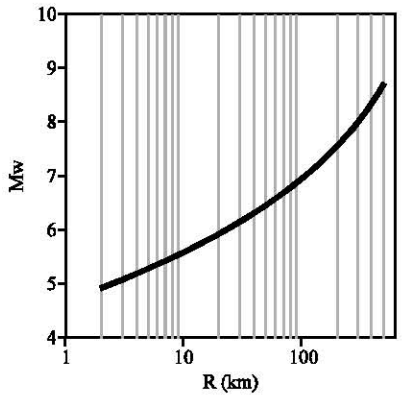

Fig. 12: Effect of surface epicenter distance on soil liquefaction ratio (Mirhosainy,1993)

Table 4: The smallest earthquake magnitudes which could cause liquefaction on the basis of surface epicenter distance

M_W	4.9	5.1	5.2	5.3	5.4	5.4	5.5	5.5	5.6
R	2	3	4	5	6	7	8	9	10

In the study area, owing to the fact that there are seismic springs located 5 to 10 km from the city of Torkaman, earthquakes with magnitudes of M_w> 5.3 are capable of producing liquefaction in the soil foundation of the city. The moment magnitude of the above-mentioned distance that would need to be reached for the occurrence of liquefaction can be obtained as follows:

On the basis of the above-mentioned relationship at different distances, the least moment magnitude for liquefaction potential can be calculated as shown in Table 4.

Due to the fact that the moment magnitude of any probable earthquake in the region is 7.5 and on the basis of Fig. 12 and Eq. 10, it can be said that the study area is located in a region with liquefaction potential (Table 5).

$$M_w = 0.4323 \text{ Ln } (R) + 4.5785 \quad (10)$$

The results of preliminary examining methods for liquefaction potential have been mentioned in Table 5. Although, the importance and weight of each method is not identical to the other methods, but all the methods can be used in order to increase the trustworthiness of the final result. The conclusion which can be drawn based on this investigation is that some of the methods cannot

Table 5: Comparison of different methods of liquefaction assessment at different depths of the selected boreholes

		Assessment methods							
Borehole No.	Depth (M)	CRR/CSR	Comparison e_c with e_0	Grain size distribution	Relative density	SPT-σ'	SPT-τ/σ'	Atterberg limits	Earthquake R
BH_1	3	P	P	P	P	P	P	P	P
	6	P	P	P	P	P	P	P	P
	9	IP	P	IP	IP	IP	IP	IP	P
	12	P	P	IP	IP	IP	IP	P	P
	15	P	P	IP	P	P	P	P	P
BH2	3	P	P	P	IP	P	P	P	P
	6	P	P	IP	IP	IP	P	P	P
	9	P	P	IP	IP	IP	IP	P	P
	12	P	P	IP	P	P	P	P	P
	15	IP	P	IP	P	P	P	IP	P
BH3	3	P	P	P	IP	IP	IP	P	P
	6	P	P	P	IP	IP	IP	P	P
	9	P	P	P	IP	IP	IP	P	P
	12	P	P	P	P	P	P	P	P
	15	P	P	IP	P	P	P	P	P
BH6	3	P	P	P	IP	IP	IP	P	P
	6	IP	P	IP	IP	IP	IP	IP	P
	9	IP	P	P	IP	IP	IP	IP	P
	12	P	P	P	P	IP	P	P	P
	15	IP	P	IP	IP	IP	IP	P	P
BH7	3	P	P	P	IP	IP	IP	P	P
	6	P	P	P	P	P	P	P	P
	9	IP	P	P	IP	IP	IP	IP	P
	12	P	P	P	P	P	P	P	P
	15	IP	P	IP	P	P	P	P	P

IP: Impossible; P: Possible

be singly used for liquefaction examination. Nevertheless, geological and field observations can also be used for more precise investigation of liquefaction potential.

- Historical observations of the area indicate that Abskun Island has submerged as a result of an abrupt earthquake. This might has happened as a result of liquefaction occurrence
- Underground water level is up in all parts of the area showing the potential of the soil to liquefy
- Sediments are recent and have been ordinarily consolidated. The values of void ratio, gradation and fine particle percentage of the soil show the potential of liquefaction
- Field observations show that the permanent movement of trains has caused some cracks on small building walls showing the occurrence of liquefaction
- Clay bands with thicknesses less than 0.5 m retards the drainage of the environment thereby increasing the pore pressure and helping the liquefaction potential of the area

CONCLUSIONS

- Results obtained using Atterberg limits, examining grain size distribution and the method of comparing cyclic stress ratio were highly correlated with one another

- From a theoretical point of view, the soil may be susceptible to liquefaction, but the occurrence of liquefaction also depends on other parameters and stress conditions in the soil at the moment of rupture
- Silt soils (ML) are more susceptible to liquefaction, but there is also liquefaction potential in clay soils (CL). The drainage conditions of soil layers can alter the process of liquefaction
- The critical liquefaction depth is at 8.5 meters and the phenomenon of liquefaction is more probable for depths up to 15 m
- Increased cementation between grains and grain connection increases the resistance of soil against liquefaction, to such an extent that, despite the existence of critical void ratio values, soil can be non-liquefiable. This is due to the existence of connection between grains
- Each of the mentioned methods has different weights in assessment of liquefaction potential and cannot singly be used for this assessment
- Superimposing of different methods and engineering judgments will be real helps in valid assessment of the liquefaction potential

REFERENCES

Al-Karni, A.A., 2007. Evaluation of liquefaction potential of the soil at the university of Jazan in Jazan city in the Southwest of Saudi Arabia. Proceedings of the World Engineering Congress, (WEC'07), Penang, Malaysia, pp: 327-334.

Alisha, K., 2004. Soil Liquefaction. Mid-America Earthquake Center and Georgia Institute of Technology, Atlanta, Georgia, USA.

Anderson, D.L., P.M. Byrne, R.H. De Vall, E. Naesgaard and D. Wijewickreme, 2005. Report geotechnical design guidelines for buildings on liquefiable sites for greater vancouver region. Greater Vancouver Liquefaction Task Force Report (GVLTR), University of British Columbia.

Balideh, S., K. Goshtasbi, H. Aghababaei, N. Khaji and H. Merzai, 2009. Seismic analysis of underground spaces to propagation of seismic waves (case study: Masjed soleiman dam cavern). J. Applied Sci., 9: 1615-1627.

Boulanger, R.W., 2002. Evaluating liquefaction resistance at high overburden stresses. Proceedings of the 3rd US.-Japan Workshop on Advanced Research on Earthquake Engineering for Dams, Department of Civil and Environmental Engineering, University of California, San Diego.

Boulanger, R.W. and I.M. Idriss, 2004. State normalization of penetration resistance and the effect of overburden stress on liquefaction resistance. Department of Civil and Environmental Engineering, University of California. http://cee.engr.ucdavis.edu/Faculty/boulanger/ PDFs/ 2004/Boulanger_Idriss_overburden_SDEE_2004.pdf.

Department of Defense, 1983. Soil Dynamics and Special Design Aspects. Association of American Publishers, USA.

Idriss, I.M. and R.W. Boulanger, 2003. Relating ká and kó to SPT Blow Count and to CPT Tip. University of California, Berkeley.

Idriss, I.M. and R.W. Boulanger, 2004. Semi-empirical procedures for evaluating liquefaction potential during earthquakes. Proceedings 11th SDEE and 3rd ICEGE, (SI'04), Berkeley, CA., pp: 484-491.

JPSCO., 2010. Report geotechnical exploration Mehr housing in Turkman city. Pars Keshesh.

Maugeri, M. and P. Monaco, 2006. Liquefaction potential evaluation by SDMT. Proceedings of 2nd International Conference on the Flat Dilatometer, (ICFD'06), Washington DC., pp: 295-305.

Mihai, P., I. Gosav and B. Rosca, 2010. Study on the earthquake action of old masonry structures. J. Applied Sci., 10: 157-165.

Mirhosainy, M. and B. Arefpoor, 2001. Geotechnical Earthquake Engineering. 1st Edn., IIEES., Tehran, Iran.

Mirhosainy, M., 1993. Soil Dynamich. IIEES., Tokyo, Japan.

Polito, C.P., 1999. The effects of non-plastic and plastic fines on the liquefaction of sandy soils. Ph.D. Thesis, Faculty of the Virginia Polytechnic Institute and State University in Partial.

Robertson, P.K., 2007. Seismic design for liquefaction summary. http://www.cpt-robertson.com/pdfs/seisdesign_liq07.pdf.

Tahooni, S., 1996. Principles of Foundation Engineering. 3rd Edn., Amirkabir University, Tehran, Iran.